EXISTENCE OF TOPOLOGICAL PHASE IN $RbCd_4As_3$: A FIRST PRINCIPLES STUDY

A PROJECT REPORT

SUBMITTED IN PARTIAL FULFILLMENT OF THE REQUIREMENTS
FOR THE AWARD OF THE DEGREE
OF

MASTER OF SCIENCE
IN
PHYSICS

Submitted by

NITIKA SACHDEVA (2K21/MSCPHY/35)

Under the supervision of

DR. MUKHTIYAR SINGH

DEPARTMENT OF APPLIED PHYSICS
DELHI TECHNOLOGICAL UNIVERSITY
(Formerly Delhi College of Engineering)
Bawana Road, Delhi 110042

MAY, 2022

DEPARTMENT OF APPLIED PHYSICS
DELHI TECHNOLOGICAL UNIVERSITY
(Formerly Delhi College of Engineering)
Bawana Road, Delhi-110042

CANDIDATE'S DECLARATION

I, NITIKA SACHDEVA, Roll No. – 2K21/MSCPHY/35 student of M.Sc Physics (Applied Physics), hereby declare that the project Dissertation titled "Existence of Topological Phase in $RbCd_4As_3$: A First-Principles Study" which is submitted by me to the Department of Applied Physics, Delhi Technological University, Delhi in partial fulfillment of the requirement for the award of the degree of Master of Science in Physics, is original and not copied from any source without proper citation. This work has not previously formed the basis for the award of any Degree, Diploma Associateship, Fellowship, or other similar title or recognition.

Title of the Paper: "Existence of Topological Phase in $RbCd_4As_3$: A First-Principles Study"

Author names: Nitika Sachdeva, Ramesh Kumar, and Dr. Mukhtiyar Singh

Name of the conference: 2nd International Hybrid Conference on Smart Grid and Electric Vehicle (ICSGEV23)

Conference Date: April 03-04, 2023

Have you registered for the conference: Yes

Status of paper: Accepted

Date of Acceptance: March 17, 2023

Place: Delhi

Date: 25.05.23 **Nitika Sachdeva (Student)**

DEPARTMENT OF APPLIED PHYSICS
DELHI TECHNOLOGICAL UNIVERSITY
(Formerly Delhi College of Engineering)
Bawana Road, Delhi-110042

CERTIFICATE

I hereby certify that the Project Dissertation titled "Existence of Topological Phase in $RbCd_4As_3$: A First Principles Study" which is submitted by Nitika Sachdeva, Roll No. – 2K21/MSCPHY/35, Applied Physics, Delhi Technological University, Delhi in partial fulfillment of the requirement for the award of the degree of Master of Science in Physics is a record of the project work carried out by the student under my supervision. To the best of my knowledge, this work has not been submitted in part or full for any Degree or Diploma to this University or elsewhere.

Place: Delhi | Dr. Mukhtiyar Singh

Date: 25.05.2023 | **SUPERVISOR**

Nitika Sachdeva

ACCEPTANCE

Electrical HITS <icsgev23@gmail.com>
to me

Mar 17, 2023, 8:40 AM

Dear Nitika Sachdeva,

Paper-ID: 144
Title: Existence of Topological Phase in RbCd4As3: A First Principles Study

Congratulations!

On behalf of the editorial board of ICSGEV-23, we are happy to inform you that your above-referenced paper has been ACCEPTED (based on the review reports) for presentation in the ICSGEV conference to be organized by Hindustan Institute of Technology and Science, Chennai, India, during 03^{rd} -4^{th} April 2023 and publication in AIP Conference Proceedings.

Please look at the reviewers' comments attached below, which are intended to help you improve your paper for final publication. You are advised to suitably address the reviewers' comments in your final paper.

An accepted paper will be published in the conference proceedings (AIP Conference Proceeding--Scopus indexed) only if the registration fee payment information accompanies the final version for at least one of the authors.

Instructions for Author(s) Registration & Payment of Reg. Fee
----

(a) One author must at least register each paper for getting it published in AIP.

Registration Fee: Rs. 8500/- for Research Scholar/Student,

Rs. 9000/- for Faculty

Mode of payment

Mode of Payment: Online Payment only.

Online transfer can be wired to the following account details:

CERTIFICATE OF PRESENTATION

HINDUSTAN
INSTITUTE OF TECHNOLOGY & SCIENCE
(DEEMED TO BE UNIVERSITY)

UNIVERSITY OF LEEDS

2nd INTERNATIONAL CONFERENCE ON SMART GRID & ELECTRIC VEHICLE (ICSGEV-2023)

03rd & 04th April 2023

Organized by

Department of Electrical & Electronics Engineering

CERTIFICATE OF PRESENTATION

This is to certify that Prof./Dr./Mr./Ms. Nitika Sachdeva of Delhi Technological University, New Delhi, Delhi-110042 has participated and presented titled Existence of Topological Phase in RbCd4As3: A First Principles Study Paper ID:144 in ICSGEV 2023 held at Hindustan Institute of Technology and Science, Chennai, India.

Dr. A. K. Parvathy
Convenor, HoD(EEE)
HITS, Chennai

Dr. S. Joseph Antony
Organizing Chair,
University of Leeds,
United Kingdom

CONFERENCE REGISTRATION

ICICI Bank

Transfer Successful

Reference ID	308219922898
Mode	IMPS
Paid to Account	HindustanInstituteofTechnologyScience 255402000000001
Amount	₹ 8500
From Account	XX-XX-XX-XX-XX-60
On	23/03/2023 19:02:32
Remarks	Registration for ICSGEV 2023

PAPER NAME

1685197328523_1685197323197_Delhi-Technological-University-Thesis-Template--1- (9).pdf

AUTHOR

Nitika

WORD COUNT

3166 Words

CHARACTER COUNT

16357 Characters

PAGE COUNT

15 Pages

FILE SIZE

3.0MB

SUBMISSION DATE

May 27, 2023 8:20 PM GMT+5:30

REPORT DATE

May 27, 2023 8:20 PM GMT+5:30

2% Overall Similarity

The combined total of all matches, including overlapping sources, for each database.

- 0% Internet database
- 1% Publications database
- Crossref database
- Crossref Posted Content database
- 1% Submitted Works database

2% Overall Similarity

Top sources found in the following databases:

- 0% Internet database
- 1% Publications database
- Crossref database
- Crossref Posted Content database
- 1% Submitted Works database

TOP SOURCES

The sources with the highest number of matches within the submission. Overlapping sources will not be displayed.

1	Sobhit Singh, QuanSheng Wu, Changming Yue, Aldo H. Romero, Alexey... Crossref	<1%
2	University of Strathclyde on 2011-03-30 Submitted works	<1%
3	Lucjan Jacak, Jurij Krasnyj, Arkadiusz Wójs. "Spin-orbit interaction in t... Crossref	<1%
4	Lecture Notes in Physics, 2003. Crossref	<1%

DEPARTMENT OF APPLIED PHYSICS
DELHI TECHNOLOGICAL UNIVERSITY
(Formerly Delhi College of Engineering)
Bawana Road, Delhi-110042

ACKNOWLEDGEMENT

I wish to express my sincerest gratitude to Dr. Mukhtiyar Singh for his continuous guidance and mentorship that he provided me during the project. He showed me the path to achieve our targets by explaining all the tasks to be done and explained to me the importance of this project as well as its industrial relevance. He was always ready to help me and clear my doubts regarding any hurdles in this project. Without his constant support and motivation, this project would not have been successful.

Place: Delhi — Nitika Sachdeva

Date: 25.05.2023

Abstract

In this work, we report topological phase in the layered arsenide $RbCd_4As_3$ using first-principles calculations. We find that $RbCd_4As_3$, have topological band inversion at Γ point, which verifies the topological nature. Also, a small spin-orbit band gap of 0.1559 eV is observed at Γ point. Further verification of the topological nature is carried out by calculating the Z_2 topological invariants. The parity product of valance bands shows non-zero value of Z_2 topological invariant. Surface density of state (SDOS) study shows existence of Dirac cone near the Fermi level. Conducting surface states near the Fermi level, as observed in SDOS, confirm the topological non-trivial nature of $RbCd_4As_3$.

Contents

LIST OF TABLES

LIST OF FIGURES

10. *FIGURE 10. (a) Band Structure of $RbCd_4As_3$ in wannier space with band gap induced at Γ due to spin-orbit coupling. Magnified image of the band gap induced at Γ point is shown. (b) Surface Density of States for (001) surface of $RbCd_4As_3$ calculated with spin-orbit coupling. Formation of a single Dirac cone is seen at Γ.*

LIST OF ABBREVIATIONS AND SYMBOLS

1. *PDOS: Partial Density of States*
2. *DOS: Density of States*
3. *E_F: Fermi Energy*
4. *TRIM: Time Reversal Invariant Momenta*
5. *SOC: Spin-Orbit Coupling*
6. *TRS: Time Reversal Symmetry*
7. *TI: Topological Insulators*
8. *TCI: Topological Crystalline Insulators*
9. *TSM: Topological Semi-Metal*
10. *TM: Topological Material*
11. *BZ: Brillion Zone*
12. *MLWF: Maximally Localized Wannier Function*
13. *DFT: Density Functional Theory*
14. *VASP: Vienna ab-initio simulation tool*
15. *PAW: Projector Augmented Wave Formalism*
16. *GGA: Generalized Gradient Approximation*
17. *PBE: Perdew-Burke Ernzehrof*
18. *E-CF: Exchange-Correlation Function*
19. *LDA: Local Density Approximation*
20. *ARPES: Angle-Resolved Photo-emission Spectroscopy*
21. *g: Genus Number*
22. *(v0: v1, v2, v3): Z_2 Invariant*
23. *a1, a2, a3: Reciprocal Primitive Lattice Vectors*

Chapter 1

INTRODUCTION

1.1 Topology

The branch of Topology deals with the attributes of a topological space under continuous deformations excluding wear and tear. A famous example is of a coffee mug and a donut. Since both have only one hole, they can be transformed into one another by stretching. This hole is an example of a topological invariant. A **Topological Invariant** is a parameter that remains constant in a topological space during a topological transformation.

FIGURE 1. Example of a Donut being topologically transformed into a Coffee Mug. Both are topologically equivalent since both have genus number = 1. [1]

The theorem governing this concept is the **Gauss-Bonnet Theorem**. If we integrate a closed surface curvature over its surface, then we get a topological invariant.

For a Torus or a sphere, the following equation is the Gauss-Bonnet Theorem Equation,

$$\int_M \kappa dA = 2\pi\chi = 2\pi(2-2g) \quad (1)$$

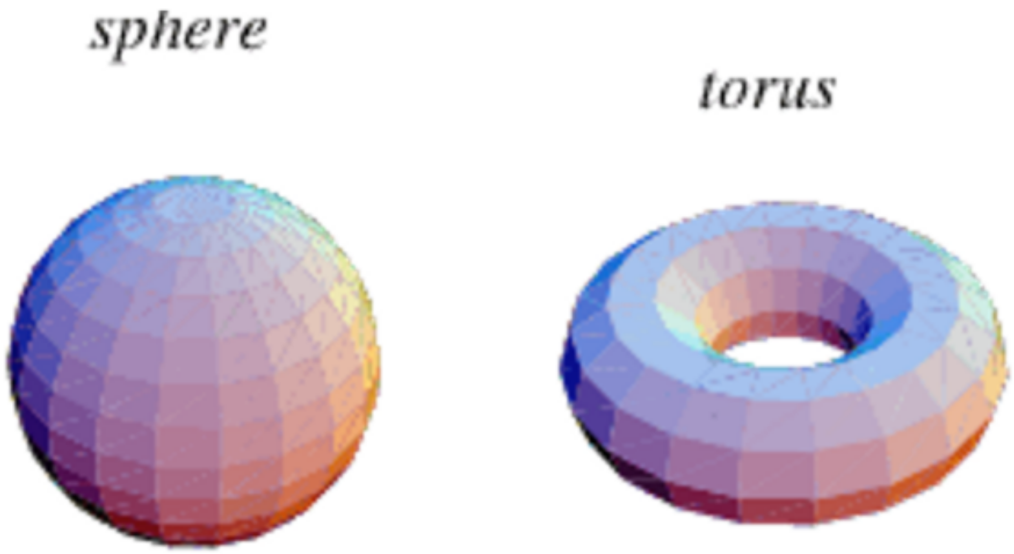

FIGURE 2. Sphere and Torus for which the above equation 1 depicts Gauss Bonnet Theorem [2]

In equation *1*, g depicts the **Genus Number** which is the number of Holes in this case, g = 0 for the sphere and g=1 for the torus. The number of holes in a topological object is always an integer. We can further understand genus number by the following image:

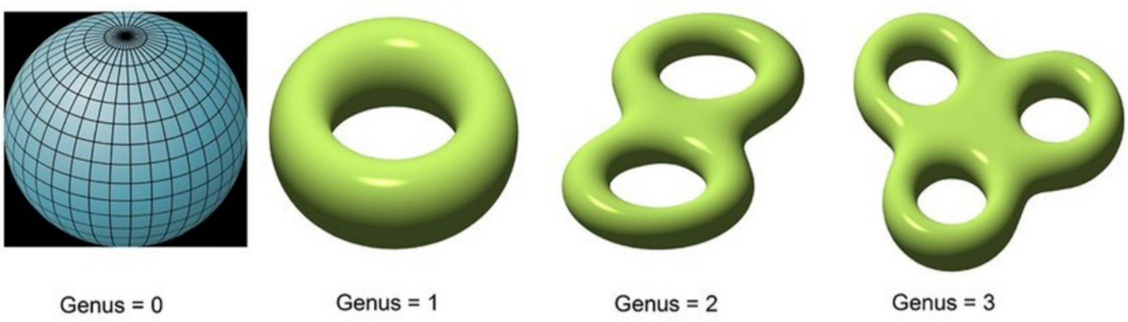

FIGURE 3. Value of g (Genus Number) for different topological surfaces, where, g depicts the number of holes. [2]

[1]

1.2 Topological Insulators

Condensed Matter Physics is the study of different states of matter based on the arrangement of electrons and atoms. Phases of matter transition into one another due to the phenomenon of *spontaneous symmetry breaking*. Symmetry is the property of matter that is invariant during transformations. Topological insulators also have these symmetries. Now, the band structure is formed when orbitals come close enough to expand and form an electronic band structure with an energy band gap in insulators. We can say that *all conventional insulators are topologically equivalent to each other* as they can be transformed into one another without losing the energy gap between the bands. This is what makes them different from trivial Insulators.

The electrons move in a circular motion due to the existence of a magnetic field in their vicinity. Though, electron bounces off the edges near the boundary forming half circles as shown in Figure 4.

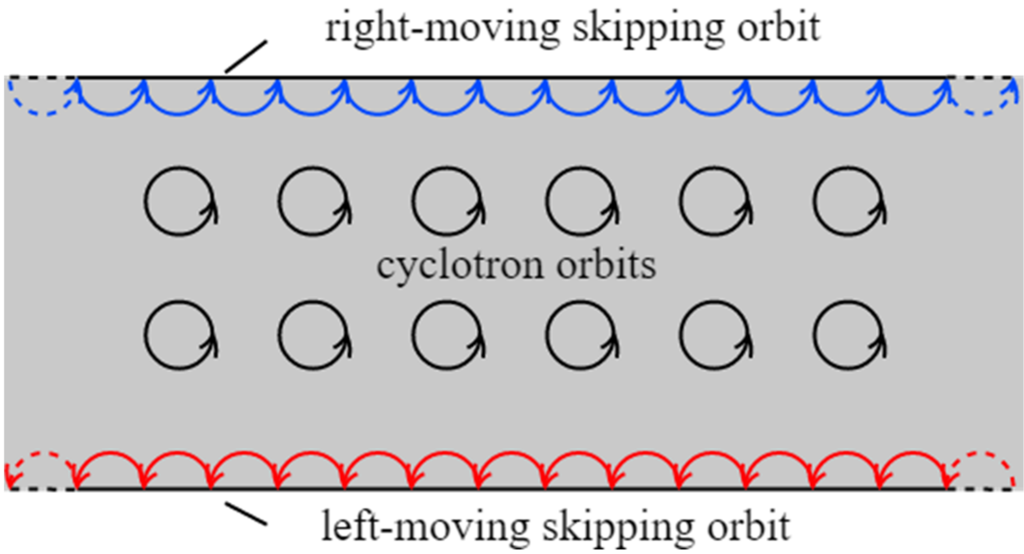

FIGURE 4. Electrons bouncing off near the edge are called the Dirac Fermions in Quantum and Skipping Orbits in Classically. The bulk electrons are in cyclotron orbits due to the presence of a magnetic field. [3]

These orbits are called **Skipping Orbits** in Classical Mechanics and **Dirac Fermions** in Quantum Mechanics. The electrons move in one direction and thus are not slowed down or obstructed by the flow of electrons in the opposite direction. At this point, **The Bulk Boundary Correspondence** comes into play which states that the bulk and boundary are connected. The *Chern Number, n*, also called the Bulk Invariant, is 0 for the insulating bulk and 1 for the Quantum Hall State. This chern number is equal to the chiral edge states of the boundary.

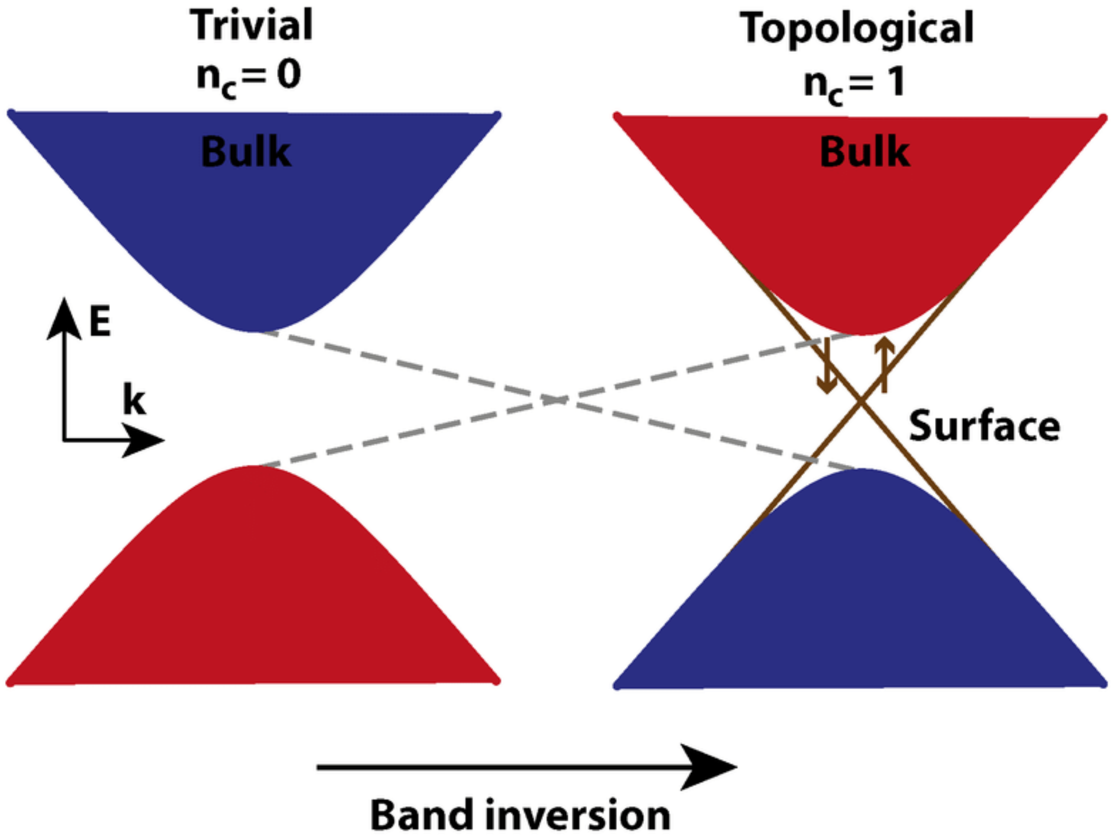

FIGURE 5. Comparison of the Band Structure of a Trivial Insulator and a Topological Insulator. The crossing across the two bands depicts the conducting edge in two-dimensional and surface states in three-dimensional samples. [4]

In Figure 5, we can see the crossing between conduction band (CB) and valence band (VB) which allows an easy pathway for the electrons to move. This edge state allows electrons to flow without dissipation, and thus the topological insulators can conduct electricity without closing the energy band gap. Also, these edge states are topologically protected, i.e. they are not distorted by deformations, just like the number of holes is protected under continuous deformation. *Thus, the edge states given by the Chern number are topological invariants, which is verified by the Bulk-Boundary theorem.*

Chapter 2

OUR WORK AND MOTIVATION

Topological Materials (TMs) have a broad application in Spintronics [5], Quantum Computing [6], Chemical Catalysis [7], and Thermoelectric Materials [8]. The phenomena exhibited by these materials such as magnetoresistance [9], chiral anomaly [10], and Weyl Fermion quantum transport [11] are increasing their popularity amongst the research community.

TMs can be divided into several categories such as Topological Semi-metals (TSM), Topological insulators (TI), Topological Crystalline Insulators (TCI), and many more. TSMs show gapless electronic states exhibiting crossing of VB and CB near the level of Fermi energy (E_F) [12]. They can be categorized into several categories such as Dirac Semi-metals, Weyl semimetals, Nodal line semimetals, and more [13-16] based on the degeneracy, co-dimension, dispersion, and origin of the band crossing. TIs have insulating bulk and gapless boundary states (2D) and gapless surface states (3D) [17-19]. Non–trivial TIs have an odd number of surface Dirac cones whereas an even number of cones makes them trivial. The non-triviality preserve Time Reversal Symmetry (TRS) and leads to some exotic properties. Other Symmetries such as crystal symmetries also conserve the quantum phenomenon in a TI and such TIs are termed as Topological Crystalline Insulators (TCIs). There are different types of TCIs that exhibit mirror symmetry as in the SnTe family [20,21] and Rotational Symmetry [22] as observed in $\alpha - Bi_4Br_4$ [23].

ARPES experimental study and Density Functional Theory (DFT) analysis of $NaCd_4As_3$ show that it has TCI characteristics at room temperature which converts to TI upon lowering the temperature [24]. Thus, the TCI conve happens due to the broken mirror symmetry[24]. Besides, $NaCd_4As_3$ have been reported as a part of two Zintl Phases series namely, DCd_4Q_3 and DZn_4Q_3 (D = Na, K, Rb, Cs; Q = As, P), in which respective elements have been used to compose 12 complex structures including layered arsenide like $NaCd_4As_3$, $NaZn_4As_3$, $NaCd_4As_3$, KCd_4As_3, and $RbCd_4As_3$ [25,26]. There are structural similarities found in these layered arsenides as established by X-ray Diffraction (XRD) [25,26]. Moreover, the stable crystal structure of $RbCd_4As_3$ has been experimentally synthesized and the calculations of the Band Energy Structure and its properties have been reported without considering the interaction between the spin and the orbital angular momentum (SOC) [25]. However, including spin-orbit interaction in band structure calculation has immoderate shifts in the topology of a material as observed in Bi_2Se_3 [27]. Even the strength of the spin-orbit interaction can be enhanced by various methods like chemical doping [28], applying a magnetic field [29], or increasing hydrostatic pressure [30].

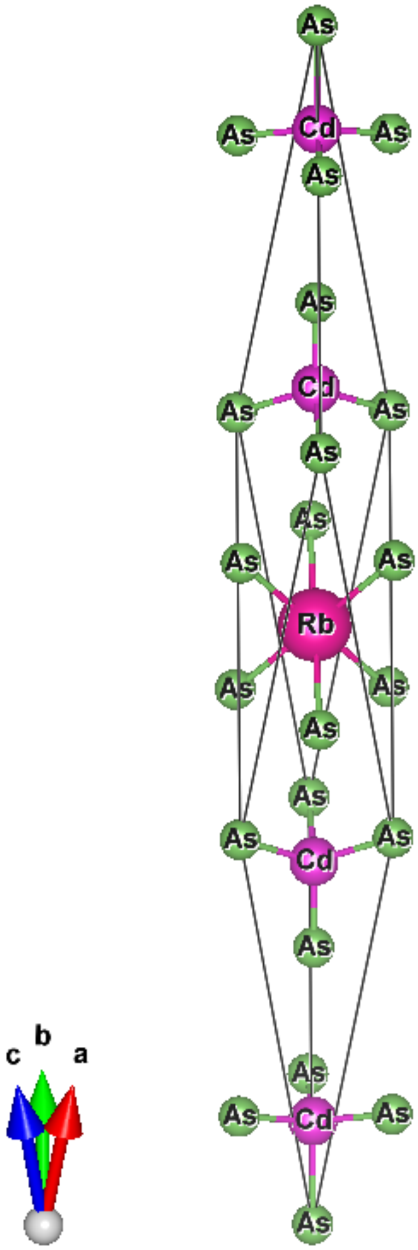

FIGURE 6. $RbCd_4As_3$

Thus, the experimental observation of topological phase transition in $NaCd_4As_3$ and the similarity of structure with $RbCd_4As_3$, makes it interesting to study the electronic and topological properties of $RbCd_4As_3$ [24-26] under the effect of SOC.

Hence, we have probed the topological structure of the material $RbCd_4As_3$ using the first-principle calculations and found that $RbCd_4As_3$ shows a topological phase with SOC. Further, the topological nature is also verified by surface states visualized in (001) plane.

Chapter 3

COMPUTATIONAL METHODOLOGY

To evaluate the band structure properties of $RbCd_4As_3$, we used the DFT calculations [31,32] as accoutered in Vienna ab-initio simulation tool (VASP) [33] such that the calculations are carried out with the projector augmented wave formalism(PAW) [34]. To include the exchange-correlation function as in PAW formalism, we used the method of first order correction in electron density, i.e., the Generalized Gradient Approximation (GGA). Further, we have used the most common functional of GGA, which is the Perdew-Burke Ernzehrof (PBE) [35,36] considering the spin-orbit coupling. The structural relaxation of $RbCd_4As_3$ is performed using the strict energy convergence criteria of 1 × 10-6 eV. To calculate structural properties and the electronic band structure, the limit of kinetic energy is set at 520 eV. To sample a Brillion Zone (BZ) in rhombohedral structure, a 7x7x3 size Gamma-centered k-mesh is used. Fermi level is broadened with a width of 0.001 eV using Gaussian smearing. We used 0.001 eV/A force for each atom to obtain the relaxed atomic structure of a unit cell. Using maximally localized Wannier Functions [37], for tight-binding models to produce the band structure under the influence of the spin-orbit interplay constructed by Wannier90 code [38]. Besides, we used the respective Wannier tools to evaluate the resultant tight-binding Hamiltonian to finally obtain the surface states of $RbCd_4As_3$ [39].

3.1 Density Functional Theory (DFT)

To deepen our understanding of many-body systems such as more than one electron atom, we imply an approximation technique called the Density Functional Theory (DFT) [40]. It is feasible to solve Schrodinger equation for a one-electron system but not for a multi-electron system. Thus, we take some approximations like:

3.1.1 Born-Oppenheimer Approximation

This assumes respective atomic nucleus to be fixed since the its motion is not as fast as an electron, rather relatively much slower.

3.1.2 Hohenberg–Kohn Theorem

According to this concept, if we consider the n = 0 state energy, then it will be the function of another function, i.e. a Functional of the electron density because to evaluate the ground state properties like the energy, momentum, and others, one can exploit electron density.

Exchange-Correlation Function (E-CF)

Electrons interact with each other via coulomb charge and their spins. All this quantum mechanical information is stored in the E-CF.

The Kohn-Sham Equations of DFT are as follows[41]:

$$[-0.5\nabla^2 + p_{ext}(x) + p_H(x) + P_{XC}(x)]\varphi_i(x) = \epsilon_i \varphi_i(x) \tag{1}$$

where, $-\frac{1}{2}\nabla^2$ denotes Kinetic Energy, $p_{ext}(x)$ depicts potential applied externally, $p_H(x)$ is a quantity named after a scientist, Hartree Potential, and $P_{XC}(x)$ is the E-C Potential .

The E-CP is given be the formula:

$$P_{XC}(x) = \frac{\delta E_{XC}}{\delta m(r)} \tag{2}$$

There are multiple Exchange-Correlation Functionals with different accuracy and feasibility as shown in the following figure:

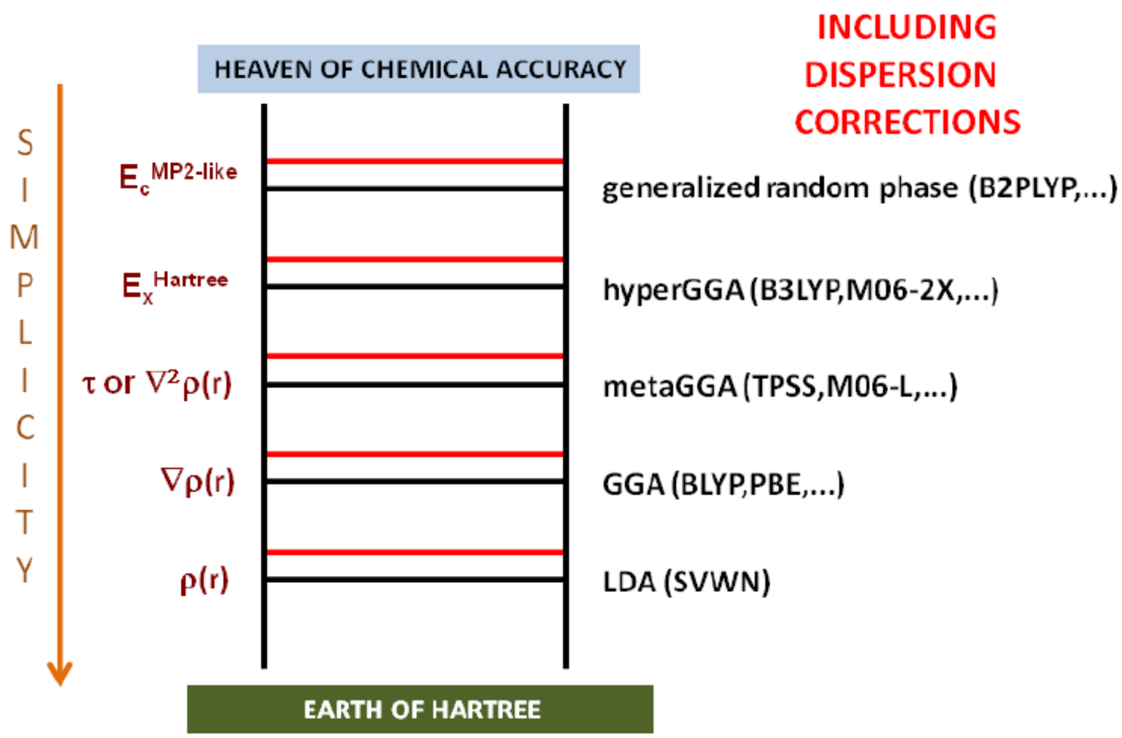

FIGURE 7. Jacobs ladder approach for the systematic improvement of DFT functionals[42]

The simplest is the Hartree approximation with the lowest accuracy. As we move up the ladder the accuracy increases towards more practical approximations. Here, **LDA** is the *Local*

Density Approximation. It takes only the electron density as a functional. It conserves the most time but is the least accurate. Next is the **GGA** Approximation which is the *Generalised Gradient Approximation*. It includes the first-order correction for Electron Density. It takes up more time than LDA but still, it is extremely fast. This is the method that we have used. Its governing equation is as follows[35]:

$$E_{EX}^{GGA} = \int \epsilon_{EX}^{GGA}(n, \nabla n) d^3 r \tag{3}$$

We have the PBE functional of the GGA Functional which is the popular choice for accurate and simple calculations in Solid State Physics[36]. In this, The parameters of the functionals are not empirically determined. Similarly, other Exchange-Correlation Functionals are MetaGGA [43,44], which takes the doubly corrected electron density, hyperGGA, and generalized random phase.

For all DFT Packages, the input of atomic positions is required. This task is done by using multiple molecule editing software like VESTA, Avogadro, etc. We have used VESTA for our molecule[45].

Chapter 4

RESULTS AND DISCUSSION

We investigate the alkali metal layered arsenide $RbCd_4As_3$ band structure for its topological nature. $RbCd_4As_3$ is experimentally synthesized in space group R$\overline{3}$m (166) in the rhombohedral phase. We took the lattice parameters a (4.4752 Å) and c (36.946 Å) from the reported experimental study [25]. For this study, we used the primitive structure to avoid band-folding with atomic positions as shown in Fig. 7(a). To understand our system, we need to evaluate the available modes for electrons around the nucleus, which is given by the projected density of states (PDOS). For our molecule $RbCd_4As_3$, the DOS can be seen in Fig. 7(b). We observe that in the valence band, the DOS majorly consists of p-orbitals of As near the fermi-level whereas the s-orbital of Cd vanishes. On the contrary, in the conduction band, both orbitals have similar contributions near 0 eV.

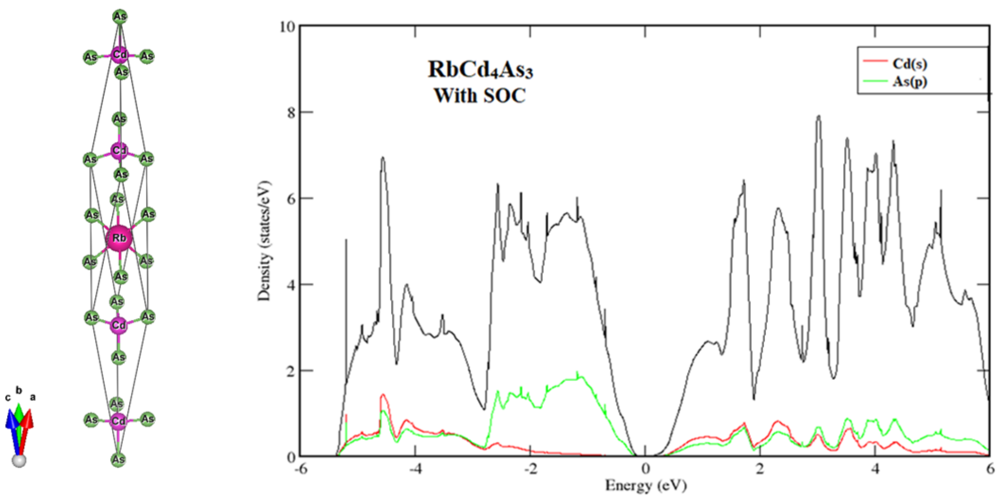

FIGURE 8. (a) Primitive Structure of $RbCd_4As_3$; (b) Projected Density of States (PDOS) of $RbCd_4As_3$ with consideration of contribution from Cd and As. The E_F is set to 0 eV

The calculation for electronic band for the cases where SOC is considered and where it isn't can be seen in Fig. 8. The band calculation is executed taking a specific path out which some points follow the equation $S + Q = -S$, where S is the Specific point which is extremely symmetric and Q is the point in the reciprocal lattice. The specific points we talk about are Γ, T, H_2, H_0 L, S_0, S_2, and F, and the points that follow this equation are found to be Γ, T, L, and F. Such points are termed as the 'Time Reversal Invariant Momenta (TRIM) Points'. Under the effect of SOC, $RbCd_4As_3$ shows topological band inversion at Γ high symmetry point. A small spin-orbit gap of 0.1559 electron-volt is also observed at one of the TRIM points, Γ. The orbital contribution of Cd(s-orbital) and As(p-orbital) is observed mainly near E_F (Fig. 8) and can also be verified with the help of projected density of states (PDOS) (Fig. 7(b)). One can also observe in the PDOS of $RbCd_4As_3$ in Fig. 7(b) that spin-orbit band gap is present. From Fig. 8(b) it can be verified that at Γ point inverted contribution of s-orbital of Cd and p-orbital of As (Fig. 8(b) inset) show topological inversion and hence non-trivial nature can be seen. No other inversion is observed on high symmetry points which confirms the existence of a single Dirac cone in $RbCd_4As_3$ and hence its topological nature.

To further investigate $RbCd_4As_3$ topology, we calculate the parity of the system at TRIM points. For 3D systems, Z_2-invariants are (ν_0: ν_1, ν_2, ν_3) whose values are governed by the following equations, as suggested by Kane and Mele [18,46,47]:

$$(-1)^{\nu_0} = \Pi_i \delta_i \tag{1}$$

$$(-1)^{\nu_{i=1,2,3}} = \Pi_{m_{j\neq i} \& m_{i=1}} \delta_{m_1 m_2 m_3} \tag{2}$$

Where $\Pi_i\ \delta_i$ denotes the parity products for filled valence bands at all TRIM points and the index value gives the class. These equations are applicable only for systems with inversion symmetry and Time Reversal Symmetry (TRS). There are eight TRIM points that can be calculated using equation (3)[18,46,47].

$$G_{i=m_1 m_2 m_3} = \frac{m_1 a_1 + m_2 a_2 + m_3 a_3}{2} \tag{3}$$

Here, m_1, m_2, m_3 can take values as 0 and 1 and they are multiplied by the reciprocal lattice points respectively. The nature or strength of the topological insulator can be determined by the value of ν_0 calculated using equation (1). For ν_0 = 1, is the sign that the molecule being considered is a good TI, whereas for ν_0 = 0, it is trivial or weak in nature. The values of ν_1, ν_2, and ν_3, given by equation (2) are used to distinguish between a weak TI and a trivial insulator. The parity for valence bands at all TRIM points for band structure calculations with spin-orbit coupling is shown in Table 1. It can be observed that the product of all TRIM points is (-). The value of the Z_2 index ν_0 as calculated from equation (1) comes out to be 1. This verifies that $RbCd_4As_3$ have strong topological nature.

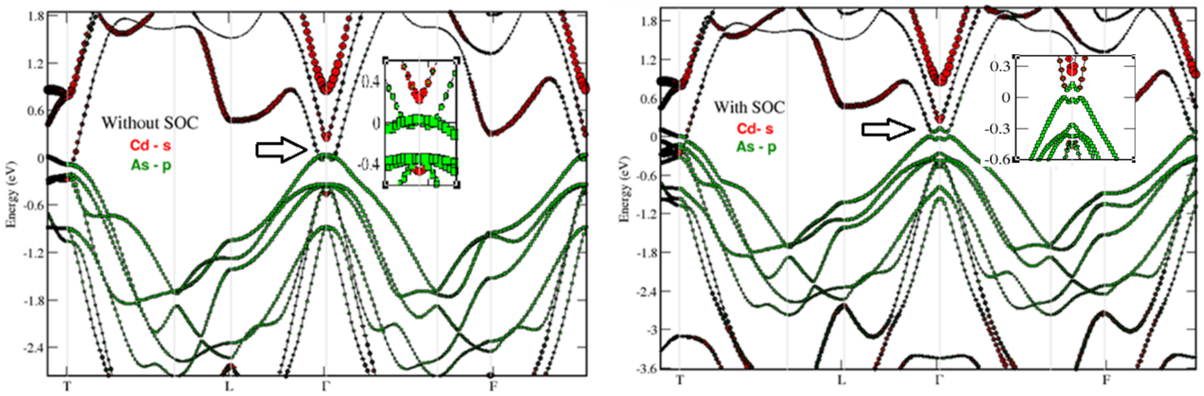

FIGURE 9. Band structures of $RbCd_4As_3$ (a) without the SOC effect and (b) with SOC. Red spheres show the contribution of Cd's s-orbital and green spheres show the contribution of the p-orbital of As atom to the bands near the E_F = 0 eV.

TRIM Points	Parity
Γ	-
3L	-
3F	-
T	+
Resultant	-

TABLE 1. Band Structure Parities at TRIM points of 1st BZ of $RbCd_4As_3$ for primitive structure with SOC.

Additionally, Bloch Energies of $RbCd_4As_3$ are utilized to get the maximally localized wannier function (MLWF) as shown in Fig. 8(b). Since the MLWFs we obtained are not dependent on the basis set used to obtain Bloch states [38], we can use them to calculate band structure in wannier space and verify the band structure obtained from Bloch states. The calculated band structure in wannier space can be observed in Fig. 9(a).

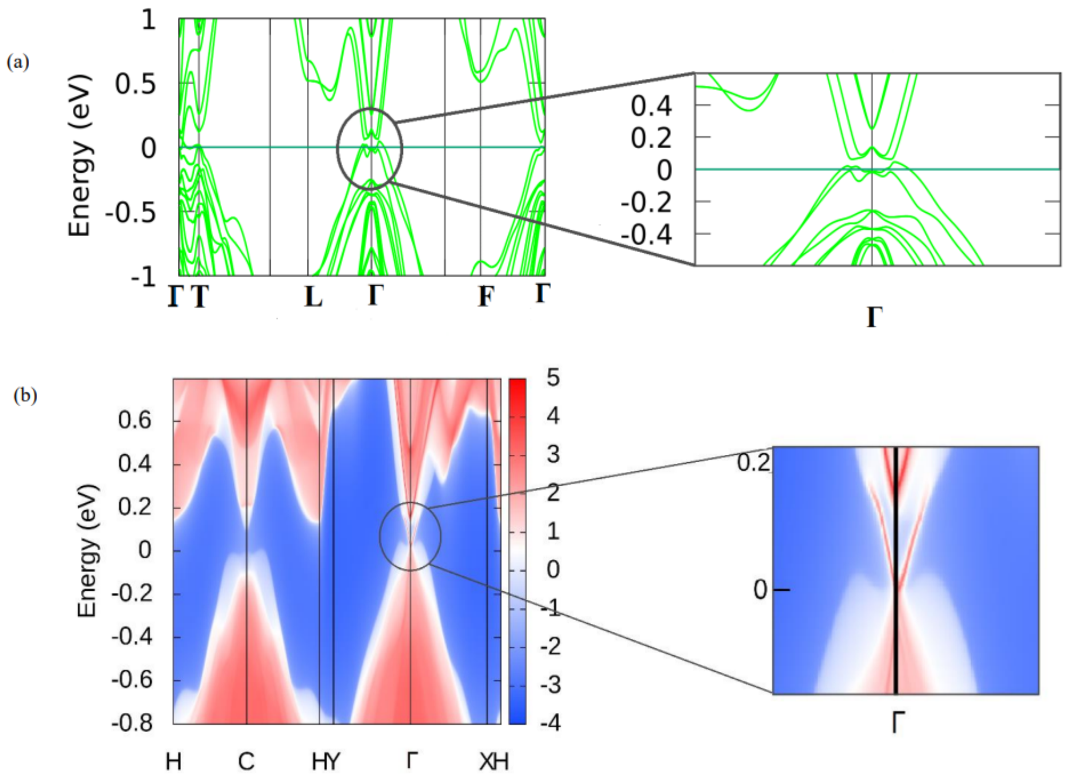

FIGURE 10. (a) Band Structure of $RbCd_4As_3$ in wannier space with band gap induced at Γ due to spin-orbit coupling. Magnified image of the band gap induced at Γ point is shown. (b) Surface Density of States for (001) surface of $RbCd_4As_3$ calculated with spin-orbit coupling. Formation of a single Dirac cone is seen at Γ.

In the Fig.9(a), a small spin-orbit energy band-gap is seen at the symmetric point Γ. This is observed in the wannier band structure and perfectly coincides with Bloch structure, thus verifying it (Fig.8(b)). Further, we used MLWFs to perform surface state calculations for (001) surface of $RbCd_4As_3$ taking into account the Green's impulse response. From our first-principle calculations, we derive a Hamiltonian to have the information of surface states. This is facilitated by a Tight-Binding Model. The resulting Surface Density of States (SDOS) forms only one cone (Dirac) at Γ as shown in Fig.9(b). This is in agreement with the spin-orbit band gap observed in Fig. 8(b) and Fig. 9(a). The presence of conducting surface state on (001) plane of $RbCd_4As_3$ is validated by looking at these figures due to odd number of Dirac cones. The existence of topological band inversion and conducting surface state along with a surface Dirac cone near the Fermi level shows that $RbCd_4As_3$ has non-trivial topological nature.

A topological insulator can generally be good thermoelectric material. $RbCd_4As_3$ is a Zintl compound and on preliminary transport calculations Zintl Compounds are suggested to be good thermoelectric materials [8]. Besides, $RbZn_{43}$ is also a member of this family and is proven to be a thermoelectric material [25]. Another member of this family is $NaCd_4As_3$, which is shown to have the desired value of variables that supports the thermoelectricity. These variables are electrical conductivity and Seebeck coefficient [25] and the existence of a topological phase is also seen with it[24], indicating a strong possibility of possessing thermoelectric properties. Hence, it would be worthwhile to investigate $RbCd_4As_3$ and other materials of this family for having thermoelectric properties for which our study can be used.

Chapter 5

CONCLUSION

Topological properties for the alkali metal layered arsenide $RbCd_4As_3$ have been studied using the DFT approximation. Also, stable rhombohedral structure with space group 166 is considered to study the band structure of $RbCd_4As_3$. We have observed a single band inversion at Γ-point under the consideration of the SOC and small spin momentum and orbit momentum interaction band gap of 0.1559 eV. The orbital contribution during the inversion can be attributed to the respective atoms Cadmium (s) and Arsenic (p). Besides, the Z_2 values are determined to verify topological phase. The multiplication result of parities computed at multiple TRIM points has shown that Z_2 index ν_0 = 1. This has suggested that $RbCd_4As_3$ is topologically non-trivial. The Surface density of the state has also verified the existence of a single Dirac cone and conducting surface state in $RbCd_4As_3$. The band inversion and surface state study of $RbCd_4As_3$ have confirmed its topologically non-trivial nature. We hope that future experimental studies will verify its topological nature as the surface state can be observed with the help of Angle-Resolved Photo-emission Spectroscopy (ARPES).

Chapter 6

PROOF OF SCOPUS INDEXING

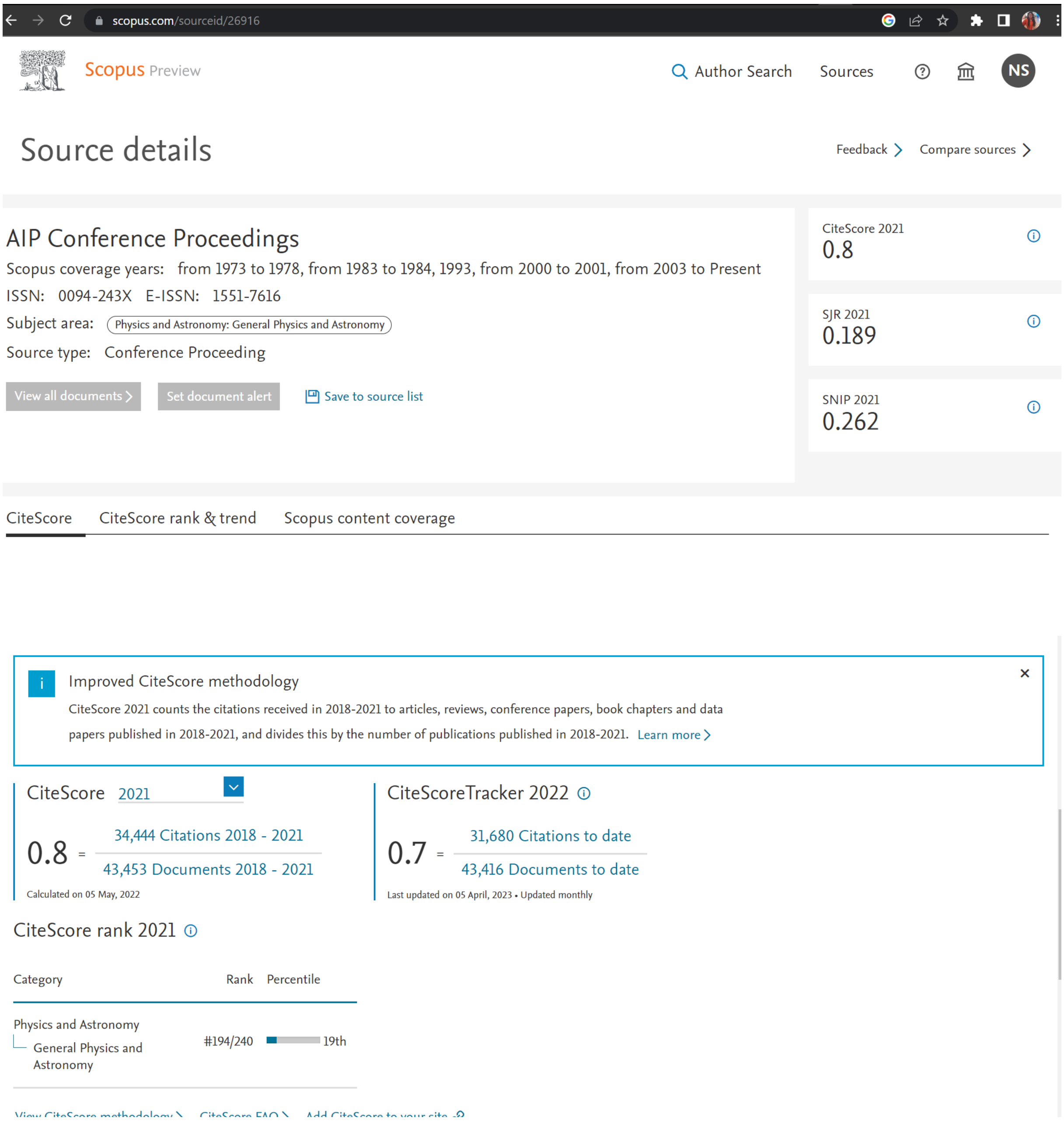

scopus.com/sourceid/26916

Scopus Preview

Author Search Sources NS

Source details

Feedback > Compare sources >

AIP Conference Proceedings

Scopus coverage years: from 1973 to 1978, from 1983 to 1984, 1993, from 2000 to 2001, from 2003 to Present

ISSN: 0094-243X E-ISSN: 1551-7616

Subject area: Physics and Astronomy: General Physics and Astronomy

Source type: Conference Proceeding

View all documents > Set document alert Save to source list

CiteScore 2021
0.8

SJR 2021
0.189

SNIP 2021
0.262

CiteScore CiteScore rank & trend Scopus content coverage

Improved CiteScore methodology

CiteScore 2021 counts the citations received in 2018-2021 to articles, reviews, conference papers, book chapters and data papers published in 2018-2021, and divides this by the number of publications published in 2018-2021. Learn more >

CiteScore 2021

0.8 = 34,444 Citations 2018 - 2021 / 43,453 Documents 2018 - 2021

Calculated on 05 May, 2022

CiteScoreTracker 2022

0.7 = 31,680 Citations to date / 43,416 Documents to date

Last updated on 05 April, 2023 • Updated monthly

CiteScore rank 2021

Category	Rank	Percentile
Physics and Astronomy — General Physics and Astronomy	#194/240	19th

Bibliography

[1] D. Thimmesch, "These 3D Printed Porcelain Coffee Mugs & Donuts are Clever Topology-Related Joke", https://www.scribbr.com/ieee/ieee-website-citation/#:~:text=To%20write%20an%20IEEE%20reference,or%20removed%20in%20the%20future. (4/24, 2023)

[2] Y. Tibrewal, "Interesting Shapes: Why is a doughnut equivalent to a coffee mug?", https://tomrocksmaths.com/2021/08/09/interesting-shapes-why-is-a-doughnut-equivalent-to-a-coffee-mug/ (4/24, 2023)

[3] Topology course team, Copyright 2021, TU Delft, CC-BY-SA 4.0 (materials) & BSD (code), "Where do the pumped electrons come from and go to?", https://topocondmat.org/w3_pump_QHE/QHEedgestates.html (4/24, 2023)

[4] M. Hakl, "Magneto-optics of relativistic-like electrons in 3D solids", https://www.researchgate.net/figure/An-illustration-of-two-types-of-the-insulator-with-different-band-orderings-trivial_fig1_322927285, (4/24, 2023)

[5] S. A. Yang, "Dirac and Weyl materials: Fundamental aspects and some spintronics applications," *SPIN*, vol. 6, no. 2. 2016. doi: 10.1142/S2010324716400038.

[6] C. Nayak, S. H. Simon, A. Stern, M. Freedman, and S. das Sarma, "Non-Abelian anyons and topological quantum computation," *Rev Mod Phys*, vol. 80, no. 3, 2008, doi: 10.1103/RevModPhys.80.1083.

[7] C. R. Rajamathi *et al.*, "Weyl Semimetals as Hydrogen Evolution Catalysts," *Advanced Materials*, vol. 29, no. 19, 2017, doi: 10.1002/adma.201606202.

[8] Sangeeta, R. Kumar, and M. Singh, "Realizing high thermoelectric performance in p-type RbZn4P3 Zintl compound: a first-principles investigation," *J Mater Sci*, vol. 57, no. 23, 2022, doi: 10.1007/s10853-022-06953-y.

[9] F. F. Tafti, Q. D. Gibson, S. K. Kushwaha, N. Haldolaarachchige, and R. J. Cava, "Resistivity plateau and extreme magnetoresistance in LaSb," *Nat Phys*, vol. 12, no. 3, 2016, doi: 10.1038/nphys3581.

[10] X. Huang *et al.*, "Observation of the chiral-anomaly-induced negative magnetoresistance: In 3D Weyl semimetal TaAs," *Phys Rev X*, vol. 5, no. 3, 2015, doi: 10.1103/PhysRevX.5.031023.

[11] A. A. Zyuzin and A. A. Burkov, "Topological response in Weyl semimetals and the chiral anomaly," *Phys Rev B Condens Matter Mater Phys*, vol. 86, no. 11, 2012, doi: 10.1103/PhysRevB.86.115133.

[12] J. Li, Z. Zhang, C. Wang, H. Huang, B. L. Gu, and W. Duan, "Topological semimetals from the perspective of first-principles calculations," *J Appl Phys*, vol. 128, no. 19, 2020, doi: 10.1063/5.0025396.

[13] H. Gao, J. W. F. Venderbos, Y. Kim, and A. M. Rappe, "Topological Semimetals from First Principles," *Annu Rev Mater Res*, vol. 49, 2019, doi: 10.1146/annurev-matsci-070218-010049.

[14] S. M. Young, S. Zaheer, J. C. Y. Teo, C. L. Kane, E. J. Mele, and A. M. Rappe, "Dirac semimetal in three dimensions," *Phys Rev Lett*, vol. 108, no. 14, 2012, doi: 10.1103/PhysRevLett.108.140405.

[15] H. Weng, C. Fang, Z. Fang, B. Andrei Bernevig, and X. Dai, "Weyl semimetal phase in noncentrosymmetric transition-metal monophosphides," *Phys Rev X*, vol. 5, no. 1, 2015, doi: 10.1103/PhysRevX.5.011029.

[16] A. A. Burkov, M. D. Hook, and L. Balents, "Topological nodal semimetals," *Phys Rev B Condens Matter Mater Phys*, vol. 84, no. 23, 2011, doi: 10.1103/PhysRevB.84.235126.

[17] B. A. Bernevig, T. L. Hughes, and S. C. Zhang, "Quantum spin hall effect and topological phase transition in HgTe quantum wells," *Science (1979)*, vol. 314, no. 5806, 2006, doi: 10.1126/science.1133734.
[18] C. L. Kane and E. J. Mele, "Z_2 Topological Order and the Quantum Spin Hall Effect," *Phys Rev Lett*, vol. 95, no. 14, 2005.
[19] M. Z. Hasan and C. L. Kane, "Colloquium: Topological insulators," *Rev Mod Phys*, vol. 82, no. 4, 2010, doi: 10.1103/RevModPhys.82.3045.
[20] T. H. Hsieh, H. Lin, J. Liu, W. Duan, A. Bansil, and L. Fu, "Topological crystalline insulators in the SnTe material class," *Nat Commun*, vol. 3, 2012, doi: 10.1038/ncomms1969.
[21] Y. Tanaka *et al.*, "Experimental realization of a topological crystalline insulator in SnTe," *Nat Phys*, vol. 8, no. 11, 2012, doi: 10.1038/nphys2442.
[22] C. Fang and L. Fu, "New classes of topological crystalline insulators having surface rotation anomaly," *Sci Adv*, vol. 5, no. 12, 2019, doi: 10.1126/sciadv.aat2374.
[23] C.-H. Hsu *et al.*, "Purely rotational symmetry-protected topological crystalline insulator α-Bi_4Br_4," *2D Mater.*, vol. 6, no. 3, 2019.
[24] Y. Y. Wang *et al.*, "Magnetotransport properties and topological phase transition in NaCd4As3," *Phys Rev B*, vol. 102, no. 11, 2020, doi: 10.1103/PhysRevB.102.115122.
[25] H. He, C. Tyson, and S. Bobev, "ChemInform Abstract: Eight-Coordinated Arsenic in the Zintl Phases RbCd4As3 and RbZn4As3: Synthesis and Structural Characterization.," *ChemInform*, vol. 42, no. 44, 2011, doi: 10.1002/chin.201144013.
[26] C. Grotz, M. Baumgartner, K. M. Freitag, F. Baumer, and T. Nilges, "Polymorphism in zintl phases ACd4Pn3: Modulated structures of NaCd4Pn3 with Pn = P, As," *Inorg Chem*, vol. 55, no. 15, 2016, doi: 10.1021/acs.inorgchem.6b01233.
[27] D. West, Y. Y. Sun, H. Wang, J. Bang, and S. B. Zhang, "Native defects in second-generation topological insulators: Effect of spin-orbit interaction on Bi_2Se_3," *Phys Rev B*, vol. 86, no. 12, 2012.
[28] A. B. Maghirang *et al.*, "Predicting two-dimensional topological phases in Janus materials by substitutional doping in transition metal dichalcogenide monolayers," *NPJ 2D Mater Appl*, vol. 3, no. 1, 2019, doi: 10.1038/s41699-019-0118-2.
[29] J. Macy *et al.*, "Magnetic field-induced non-trivial electronic topology in Fe3−xGeTe2," *Appl Phys Rev*, vol. 8, no. 4, 2021, doi: 10.1063/5.0052952.
[30] M. Singh, R. Kumar, and R. K. Bibiyan, "Pressure-induced topological phase transition in XMR material YbAs: a first-principles study," *Eur Phys J Plus*, vol. 137, no. 5, May 2022, doi: 10.1140/epjp/s13360-022-02841-1.
[31] A. K. Rajagopal and J. Callaway, "Inhomogeneous electron gas," *Phys Rev B*, vol. 7, no. 5, 1973, doi: 10.1103/PhysRevB.7.1912.
[32] W. Kohn and L. J. Sham, "Self-consistent equations including exchange and correlation effects," *Physical Review*, vol. 140, no. 4A, 1965, doi: 10.1103/PhysRev.140.A1133.
[33] G. Kresse and J. Furthmüller, "Efficient iterative schemes for ab initio total-energy calculations using a plane-wave basis set," *Phys Rev B Condens Matter Mater Phys*, vol. 54, no. 16, 1996, doi: 10.1103/PhysRevB.54.11169.
[34] D. Joubert, "From ultrasoft pseudopotentials to the projector augmented-wave method," *Phys Rev B Condens Matter Mater Phys*, vol. 59, no. 3, 1999, doi: 10.1103/PhysRevB.59.1758.
[35] J. P. Perdew, K. Burke, and M. Ernzerhof, "Generalized gradient approximation made simple," *Phys Rev Lett*, vol. 77, no. 18, 1996, doi: 10.1103/PhysRevLett.77.3865.

[36] J. P. Perdew *et al.*, “Atoms, molecules, solids, and surfaces: Applications of the generalized gradient approximation for exchange and correlation,” *Phys Rev B*, vol. 46, no. 11, 1992, doi: 10.1103/PhysRevB.46.6671.
[37] N. Marzari and D. Vanderbilt, “Maximally localized generalized Wannier functions for composite energy bands,” *Phys Rev B Condens Matter Mater Phys*, vol. 56, no. 20, 1997, doi: 10.1103/PhysRevB.56.12847.
[38] A. A. Mostofi *et al.*, “An updated version of wannier90: A tool for obtaining maximally-localised Wannier functions,” *Comput Phys Commun*, vol. 185, no. 8, 2014, doi: 10.1016/j.cpc.2014.05.003.
[39] Q. S. Wu, S. N. Zhang, H. F. Song, M. Troyer, and A. A. Soluyanov, “WannierTools: An open-source software package for novel topological materials,” *Comput Phys Commun*, vol. 224, 2018, doi: 10.1016/j.cpc.2017.09.033.
[40] R. G. Parr and Y. Weitao, “Density-Functional Theory of Atoms and Molecules (International Series of Monographs on Chemistry),” *Breslow, R*, 1994.
[41] J. Toda, “Density functional treatment of interactions and chemical reactions at surfaces”, https://www.researchgate.net/figure/Jacobs-ladder-approach-for-the-systematic-improvement-of-DFT-functionals-according-to_fig1_235990497, 04/24, 2023
[42] Z. H. Yang, H. Peng, J. Sun, and J. P. Perdew, “More realistic band gaps from meta-generalized gradient approximations: Only in a generalized Kohn-Sham scheme,” Phys Rev B, vol. 93, no. 20, 2016, doi: 10.1103/PhysRevB.93.205205.
[43] J. Sun, A. Ruzsinszky, and J. Perdew, “Strongly Constrained and Appropriately Normed Semilocal Density Functional,” Phys Rev Lett, vol. 115, no. 3, 2015, doi: 10.1103/PhysRevLett.115.036402.
[44] K. Momma and F. Izumi, “VESTA3 for three-dimensional visualization of crystal, volumetric and morphology data”, Journal of Applied Crystallography, vol. 44, no. 6, 2011, doi: 10.1107/S0021889811038970
[45] L. Fu and C. L. Kane, “Topological insulators with inversion symmetry,” *Phys Rev B Condens Matter Mater Phys*, vol. 76, no. 4, 2007, doi: 10.1103/PhysRevB.76.045302.
[46] L. Fu, C. L. Kane, and E. J. Mele, “Topological insulators in three dimensions,” *Phys Rev Lett*, vol. 98, no. 10, 2007, doi: 10.1103/PhysRevLett.98.106803.

Existence of Topological Phase in $RbCd_4As_3$: A First Principles Study

Nitika Sachdeva*, Ramesh Kumar and Mukhtiyar Singh*

Delhi Technological University, New Delhi, Delhi-110042

**Corresponding author: mukhtiyarsingh@dtu.ac.in, sachnitika13@gmail.com*

Abstract. In this work, we report topological phase in the layered arsenide $RbCd_4As_3$ using *first-principles* calculations. We find that $RbCd_4As_3$, have topological band inversion at Γ point, which verifies the topological nature. Also, a small spin-orbit band gap of 0.1559 eV is observed at Γ point. Further verification of the topological nature is carried out by calculating the Z_2 topological invariants. The parity product of valance bands shows non-zero value of Z_2 topological invariant. Surface density of state (SDOS) study shows existence of Dirac cone near the Fermi level. Conducting surface states near the Fermi level, as observed in SDOS, confirm the topological non-trivial nature of $RbCd_4As_3$.

INTRODUCTION

Topological Materials (TMs) have a broad application in Spintronics[1], Quantum Computing[2], Chemical Catalysis[3], and Thermoelectric Materials[4]. The phenomena exhibited by these materials such as magnetoresistance[5], chiral anomaly [6], and Weyl Fermion quantum transport [7] are increasing their popularity amongst the research community. TMs can be divided into several categories such as Topological Semi-metals (TSM), Topological insulators (TI), Topological Crystalline Insulator (TCI) and many more. TSMs show gapless electronic states exhibiting crossing of valence and conduction bands near the Fermi level (E_F)[8]. They can be categorised into several categories such as Dirac Semi-metals, Weyl semimetals, nodal line semimetals, and more[9–12] based on the degeneracy, co-dimension, dispersion, and origin of the band crossing.

TIs have an insulating bulk and gapless boundary states (2D) and gapless surface states (3D)[13–15]. Non–trivial TIs have odd number of surface Dirac cones whereas even number of cones make them trivial. The non-triviality preserve Time Reversal Symmetry (TRS) and leads to some exotic properties. Another class of TIs in which surface states are protected by crystal symmetries instead of TRS named as topological crystalline insulators (TCIs). There are different types of TCIs which exhibit mirror symmetry as in SnTe family[16,17] and Rotational Symmetry[18] as observed in α-Bi_4Br_4[19]. ARPES experimental study and Density Functional Theory (DFT) analysis of $NaCd_4As_3$ show that it has TCI characteristics at room temperature which converts to TI upon lowering the temperature[20]. This happens due to the broken mirror symmetry leading to a topological phase transition from TCI to TI[20]. Besides, $NaCd_4As_3$ have been reported as a part of two Zintl Phases series namely, ACd_4Pn_3 and AZn_4Pn_3 (A = Na, K, Rb, Cs; Pn = As, P), in which 12 complex compounds have been synthesized from respective elements including layered arsenide like $NaCd_4As_3$, $NaZn_4As_3$, $NaCd_4As_3$, KCd_4As_3, and $RbCd_4As_3$[21,22]. There are structural similarities found in these layered arsenide as established by X-ray Diffraction (XRD) [21,22]. Moreover, the stable crystal structure of $RbCd_4As_3$ have been experimentally synthesized and its electronic structure calculations using the linear muffin-tin orbital (LMTO) method have been reported without considering the effect of spin orbit coupling (SOC)[21]. However, including spin-orbit interaction in band structure calculation can have drastic effects on the properties (topological) of a material as observed in Bi_2Se_3[23]. Even the strength of the spin-orbit interaction can be enhanced by various methods like chemical doping[24], applying magnetic field[25], or increasing hydro-static pressure[26].

Thus, the experimental observation of topological phase transition in $NaCd_4As_3$ and the similarity of structure with $RbCd_4As_3$, makes it interesting to study the electronic and topological properties of $RbCd_4As_3$[20–22] under the effect of SOC. Hence, we have probed the topological structure of the material $RbCd_4As_3$ using the *first-principle* calculations and found that $RbCd_4As_3$ shows topological phase with SOC. Further the topological nature is also verified by surface states visualised in (001) plane.

COMPUTATIONAL DETAILS

To evaluate the structural and electronic properties of $RbCd_4As_3$, we used the Density Functional Theory (DFT) calculations[27,28] as implemented in Vienna ab-initio simulation package (VASP)[29] with projector augmented wave formalism (PAW)[30]. To include the exchange-correlation function as in PAW formalism, we used the Generalized gradient approximation (GGA) of Perdew-Burke Ernzehrof (PBE)[31,32] with spin-orbit coupling. The structural relaxation of $RbCd_4As_3$ is performed using the strict energy convergence criteria of 1×10^{-6} eV . To calculate structural properties and the electronic band structure, the kinetic energy cut-off of 520 eV is used. For a sampling of Brillion Zone (BZ) in rhombohedral structure, a 7x7x3 size Gamma centered k-mesh is used. Fermi level is broadened with a width of 0.001 eV using Gaussian smearing. All atoms in the unit cell are relaxed with the force of 0.001 eV/A per atom. Using maximally localized Wannier Functions[33], for tight-binding models to produce the band structure under effect of spin orbit coupling (SOC) constructed by Wannier90 code[34]. The resultant tight binding Hamiltonian is used to calculate the surfaces states of $RbCd_4As_3$ using Wannier tools[35].

RESULTS AND DISCUSSION

We investigate the electronic structure of the alkali metal layered arsenide $RbCd_4As_3$ for topological nature. $RbCd_4As_3$ is experimentally synthesized in space group $R\bar{3}m$ (166) in the rhombohedral phase. We took the lattice parameters a (4.4752 Å) and c (36.946 Å) from the reported experimental study[21]. For this study, we used the primitive structure to avoid band-folding with atomic positions as shown in Fig. 1(a). To understand our system, we have plotted the projected density of states (PDOS) or atom-resolved density of states for $RbCd_4As_3$ in Fig. 1(b). We observe that in the valence band the DOS majorly consists of *p-orbitals* of As near the fermi level whereas the *s-orbital* of Cd vanishes. On the contrary, in the conduction band both orbitals have similar contribution near the fermi level.

The band structure calculation with and without SOC is shown in Fig. 2. The band structure calculation is performed along high symmetry path Γ, T, H_2, H_0 L, S_0, S_2, and F out of which Γ, T, L, and F are the Time reversal Invariant Momenta (TRIM) points. Under the effect of SOC, $RbCd_4As_3$ shows topological band inversion at Γ high symmetry point. A small spin orbit band gap of 0.1559 eV is also observed at Γ point. The orbital contribution of *Cd(s-orbital)* and *As(p-orbital)* is observed mainly near E_F (Fig. 2) and can also be verified with the help of projected density of states (PDOS) as shown in Fig. 1(b). The spin orbit band gap can also be observed in PDOS of $RbCd_4As_3$ as shown in Fig. 1(b). From Fig. 2(b) it can be verified that at Γ point inverted contribution of *s-orbital* of Cd and *p-orbital* of As (Fig. 2(b) inset) show topological inversion and hence non-trivial nature can be seen. No other inversion is observed on high symmetry points which confirm the existence of single Dirac cone in $RbCd_4As_3$ and hence its topological nature.

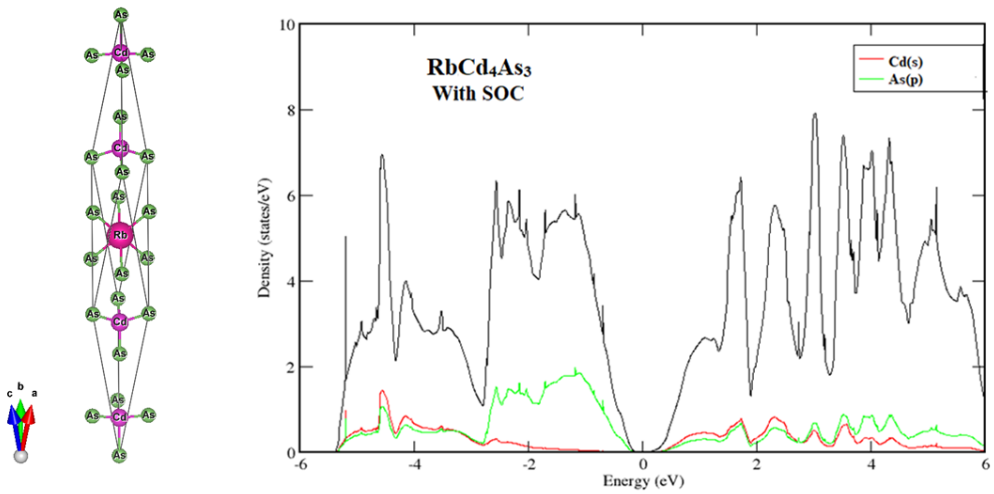

(a) (b)

FIGURE 1. (a) Primitive Structure of $RbCd_4As_3$; (b) Projected Density of States (PDOS) of $RbCd_4As_3$ with consideration of contribution from *s-orbital* of Cd and *p-orbital* of As. The Fermi level is set to 0 eV.

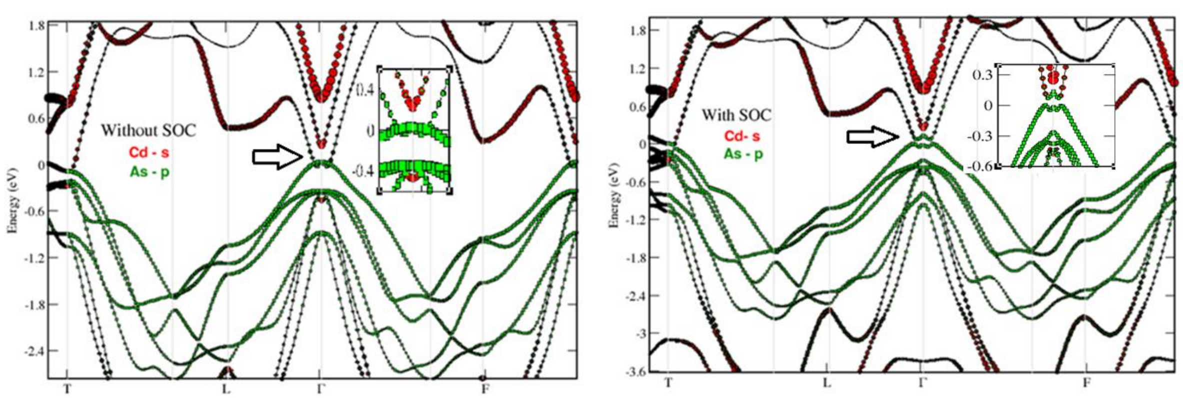

(a) (b)

FIGURE 2. Band structures of $RbCd_4As_3$ (a) without the SOC effect and (b) with SOC. Red spheres show the contribution of *s-orbital* of Cd atom and green spheres show the contribution of *p-orbital* of As atom to the bands near the Fermi level. The Fermi level is set to 0 eV.

To further investigate the topological character of $RbCd_4As_3$, we calculate the parity of the system at TRIM points. For 3D systems there are four Z_2-invariants namely (ν_0: ν_1, ν_2, ν_3) whose values are governed by the following equations as suggested by Kane and Mele[14,36,37]:

$$(-1)^{\nu_0} = \prod_i \delta_i \tag{1}$$

$$(-1)^{\nu_{i=1,2,3}} = \prod_{m_{j\neq i} \& m_{i=1}} \delta_{m_1 m_2 m_3} \tag{2}$$

Where, $\prod_i \delta_i$ denotes the parity products for filled valence bands at all TRIM points and the index value gives the class. These equations are applicable only for systems with inversion symmetry and Time Reversal Symmetry (TRS). There are eight TRIM points which can be calculated using the equation (3)[14,36,37].

$$G_{i=m_1 m_2 m_3} = \frac{m_1 a_1 + m_2 a_2 + m_3 a_3}{2} \tag{3}$$

Here, m_j= 0, 1 and a_1, a_2, a_3 are the reciprocal primitive lattice vectors. The nature or strength of the topological insulator can be determined by the value of ν_0 calculated using equation (1). For ν_0=1, the system is a strong topological insulator and for ν_0 = 0, it is trivial or weak in nature. The values of ν_1, ν_2, ν_3, given by equation (2) are used to distinguish between a weak TI and trivial insulator. The parity for valence bands at all TRIM points for band structure calculations with spin orbit coupling is shown in table 1. It can be observed that the product of all TRIM point is (-). The value of the Z_2 index ν_0 as calculated from equation (1) comes out to be 1. This verifies that $RbCd_4As_3$ have strong topological nature.

TABLE 1. Parities of all the occupied bands at TRIM points of first BZ of $RbCd_4As_3$ in primitive structure with spin-orbit coupling.

TRIM Points	Parity
Γ	-
3L	-
3F	-
T	+
Total	-

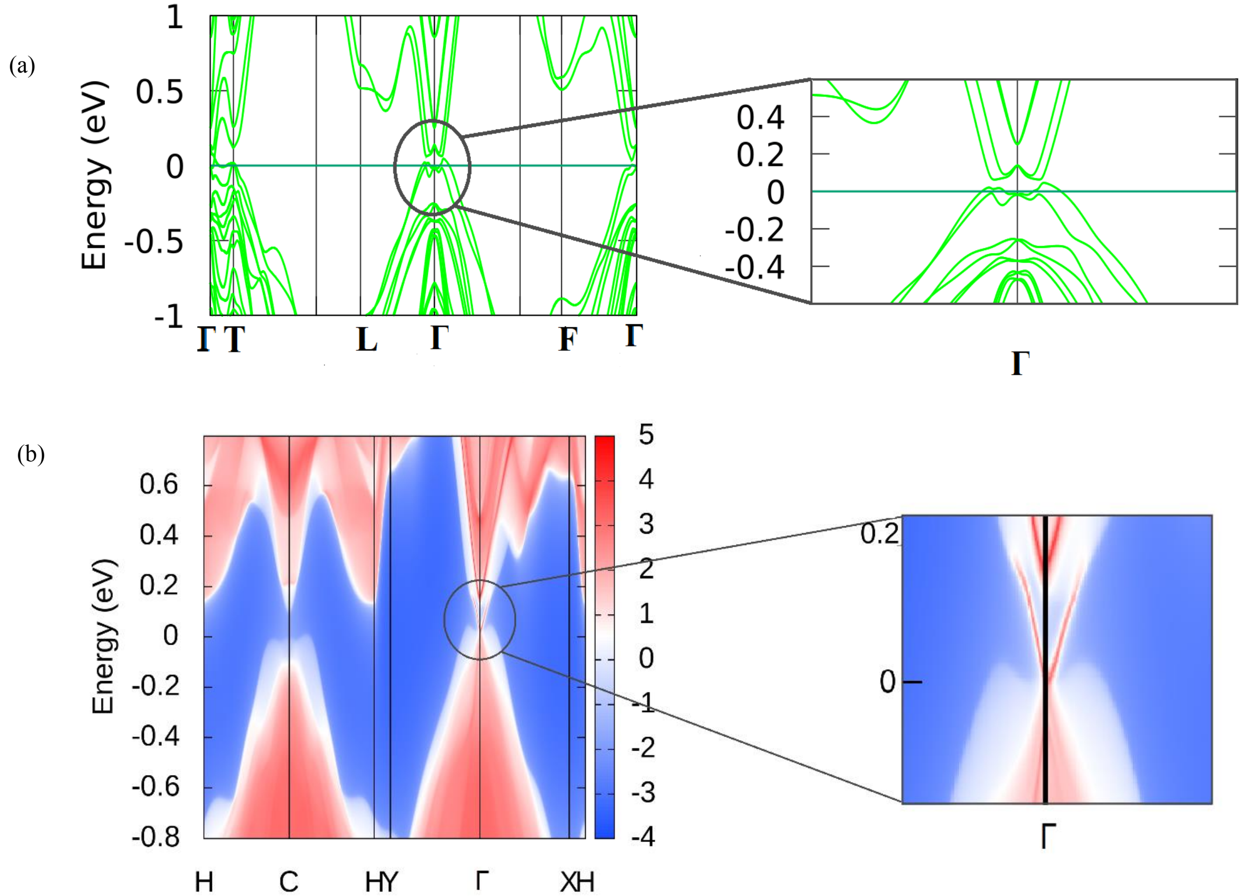

FIGURE 3. (a) Band Structure of $RbCd_4As_3$ in wannier space with band gap induced at Γ due to spin-orbit coupling. Magnified image of the band gap induced at Γ point is shown. (b) Surface Density of States for (001) surface of $RbCd_4As_3$ calculated with spin-orbit coupling. Formation of a single Dirac cone can be observed at Γ point.

Additionally, we calculate maximally localized wannier function (MLWF) from the Bloch energy bands of $RbCd_4As_3$ shown in Fig. 2(b). Since, the MLWFs are independent of the basis set used to obtain the bloch states[34], we can use them to calculate band structure in wannier space and verify the band structure obtained from Bloch states. The calculated band structure in wannier space can be observed in Fig. 3(a). The wannier band structure of $RbCd_4As_3$ (Fig.3(a)) exhibits a spin orbit band gap at *Γ-point* and perfectly coincides with the Bloch band structure, thus verifying it (Fig.2(b)). Further, we used MLWFs to perform surface state calculations for (001) surface of $RbCd_4As_3$ using the green's function approach. From our *first-principle* calculations, we derive a tight-binding model Hamiltonian to calculate the surface states. The resulting Surface Density of States (SDOS) forming a single Dirac cone at *Γ-point* is shown in Fig.3(b). This is in agreement with the spin orbit band gap observed at Γ point in Fig. 2(b) and Fig. 3(a). The presence of odd number of Dirac cones on the (001) surface of $RbCd_4As_3$ confirms the presence of conducting surface state on (001) plane of $RbCd_4As_3$.The existence of topological band inversion and conducting surface state along with a surface Dirac cone near Fermi level shows that $RbCd_4As_3$ has non-trivial topological nature. A topological insulator can generally be good thermoelectric material. $RbCd_4As_3$ is a Zintl compound and on preliminary transport calculations Zintl Compounds are suggested to be good thermoelectric materials[21]. Besides, $RbZn_4P_3$ is also a member of this family and is proven to be a thermoelectric material[4]. Another member of this family is $NaCd_4As_3$, which is shown to have a favorable combination of electrical conductivity and Seebeck coefficient[21] along with existence of a topological phase[20], indicating a strong possibility of possessing thermoelectric properties. Hence, it would be worthwhile to investigate $RbCd_4As_3$ and other materials of this family for having thermoelectric properties for which our study can be used.

CONCLUSION

The topological properties of the alkali metal layered arsenide $RbCd_4As_3$ have been studied based on the *first-principles* density functional theory calculations. The stable rhombohedral structure with space group 166 is considered to study the band structure of $RbCd_4As_3$. We have observed a single band inversion at *Γ-point* under the consideration of spin-orbit coupling effect and a small spin-orbit band gap of 0.1559 eV. The orbital contribution during the inversion can be attributed to *s-orbital* of Cd and *p-orbital* of As. We have also calculated the Z_2 topological invariants to verify the topological phase. The product of parities of all occupied bands have shown that the value of Z_2 index $\nu_0 = 1$. This have suggested that $RbCd_4As_3$ is topologically non-trivial. The Surface density of state have also verified the existence of single Dirac cone and conducting surface state in $RbCd_4As_3$. The band inversion and surface state study of $RbCd_4As_3$ have confirmed its topologically non-trivial nature. We hope that the future experimental studies will verify its topological nature as the surface state can be observed with the help of Angle Resolved Photoemission Spectroscopy (ARPES).

ACKNOWLEDGEMENT

We acknowledge National Supercomputing Mission (NSM) for providing computing resources of 'PARAM SMRITI' at NABI, Mohali, which is implemented by C-DAC and supported by the Ministry of Electronics and Information Technology (MeitY) and Department of Science and Technology (DST), Government of India.

REFERENCES

1. S.A. Yang, SPIN **6**, 1640003 (2016).
2. C. Nayak, S.H. Simon, A. Stern, M. Freedman, and S. das Sarma, Rev Mod Phys **80**, 1083-1159 (2008).
3. C.R. Rajamathi, U. Gupta, N. Kumar, H. Yang, Y. Sun, V. Süß, C. Shekhar, M. Schmidt, H. Blumtritt, P. Werner, B. Yan, S. Parkin, C. Felser, and C.N.R. Rao, Advanced Materials **29**, 1606202 (2017).
4. Sangeeta, R. Kumar, and M. Singh, J Mater Sci **57**, 10691–10701 (2022).
5. F.F. Tafti, Q.D. Gibson, S.K. Kushwaha, N. Haldolaarachchige, and R.J. Cava, Nat Phys **12**, 272–277 (2016).
6. X. Huang, L. Zhao, Y. Long, P. Wang, D. Chen, Z. Yang, H. Liang, M. Xue, H. Weng, Z. Fang, X. Dai, and G. Chen, Phys Rev X **5**, 031023 (2015).
7. A.A. Zyuzin and A.A. Burkov, Phys Rev B Condens Matter Mater Phys **86**, 115133 (2012).
8. J. Li, Z. Zhang, C. Wang, H. Huang, B.L. Gu, and W. Duan, J Appl Phys **128**, 191101 (2020).

9. H. Gao, J.W.F. Venderbos, Y. Kim, and A.M. Rappe, Annu Rev Mater Res **49**, 153-183 (2019).
10. S.M. Young, S. Zaheer, J.C.Y. Teo, C.L. Kane, E.J. Mele, and A.M. Rappe, Phys Rev Lett **108**, 140405 (2012).
11. H. Weng, C. Fang, Z. Fang, B. Andrei Bernevig, and X. Dai, Phys Rev X **5**, 011029 (2015).
12. A.A. Burkov, M.D. Hook, and L. Balents, Phys Rev B Condens Matter Mater Phys **84**, 235126 (2011).
13. B.A. Bernevig, T.L. Hughes, and S.C. Zhang, Science (1979) **314**, 1757-1761 (2006).
14. C.L. Kane and E.J. Mele, Phys Rev Lett **95**, 146802 (2005).
15. M.Z. Hasan and C.L. Kane, Rev Mod Phys **82**, 3045-3067 (2010).
16. T.H. Hsieh, H. Lin, J. Liu, W. Duan, A. Bansil, and L. Fu, Nat Commun **3**, 982 (2012).
17. Y. Tanaka, Z. Ren, T. Sato, K. Nakayama, S. Souma, T. Takahashi, K. Segawa, and Y. Ando, Nat Phys **8**, 800–803 (2012).
18. C. Fang and L. Fu, Sci Adv **5**, eaat2374 (2019).
19. C.-H. Hsu, X. Zhou, Q. Ma, N. Gedik, A. Bansil, V.M. Pereira, H. Lin, L. Fu, S.-Y. Xu, and T.-R. Chang, 2D Mater. **6**, 031004 (2019).
20. Y.Y. Wang, C. Zhong, M. Li, W.L. Zhu, W.J. Hou, W.H. Song, Q.X. Dong, Y.F. Huang, S. Zhang, Z.A. Ren, S. Wang, and G.F. Chen, Phys Rev B **102**, 115122 (2020).
21. H. He, C. Tyson, and S. Bobev, ChemInform **42**, 8375–8383 (2011).
22. C. Grotz, M. Baumgartner, K.M. Freitag, F. Baumer, and T. Nilges, Inorg Chem **55**, 7764–7776 (2016).
23. D. West, Y.Y. Sun, H. Wang, J. Bang, and S.B. Zhang, Phys Rev B **86**, 121201(R) (2012).
24. A.B. Maghirang, Z.Q. Huang, R.A.B. Villaos, C.H. Hsu, L.Y. Feng, E. Florido, H. Lin, A. Bansil, and F.C. Chuang, NPJ 2D Mater Appl **3**, 35 (2019).
25. J. Macy, D. Ratkovski, P.P. Balakrishnan, M. Strungaru, Y.C. Chiu, A. Flessa Savvidou, A. Moon, W. Zheng, A. Weiland, G.T. McCandless, J.Y. Chan, G.S. Kumar, M. Shatruk, A.J. Grutter, J.A. Borchers, W.D. Ratcliff, E.S. Choi, E.J.G. Santos, and L. Balicas, Appl Phys Rev **8**, 041401 (2021).
26. M. Singh, R. Kumar, and R.K. Bibiyan, Eur Phys J Plus **137**, 633 (2022).
27. A.K. Rajagopal and J. Callaway, Phys Rev B, **7**, 1912-1919 (1973).
28. W. Kohn and L.J. Sham, Physical Review **140**, A1133-A1138 (1965).
29. G. Kresse and J. Furthmüller, Phys Rev B Condens Matter Mater Phys **54**, 11169-11186 (1996).
30. G. Kresse and D. Joubert, Phys Rev B Condens Matter Mater Phys **59**, 1758-1775 (1999).
31. J.P. Perdew, K. Burke, and M. Ernzerhof, Phys Rev Lett **77**, 3865-3868 (1996).
32. J.P. Perdew, J.A. Chevary, S.H. Vosko, K.A. Jackson, M.R. Pederson, D.J. Singh, and C. Fiolhais, Phys Rev B **46**, 6671-6687 (1992).
33. N. Marzari and D. Vanderbilt, Phys Rev B Condens Matter Mater Phys **56**, 12847-12865 (1997).
34. A.A. Mostofi, J.R. Yates, G. Pizzi, Y.S. Lee, I. Souza, D. Vanderbilt, and N. Marzari, Comput Phys Commun **185**, 2309-2310 (2014).
35. Q.S. Wu, S.N. Zhang, H.F. Song, M. Troyer, and A.A. Soluyanov, Comput Phys Commun **224**, 405-416 (2018).
36. L. Fu and C.L. Kane, Phys Rev B Condens Matter Mater Phys **76**, 045302 (2007).
37. L. Fu, C.L. Kane, and E.J. Mele, Phys Rev Lett **98**, 106803 (2007).